Recovery of mouse neuromuscular junctions from single and repeated injections of botulinum neurotoxin A

A. A. Rogozhin[1], K. K. Pang[2], E. Bukharaeva[3], C. Young[2] and C. R. Slater[2]

[1]*Kazan State Medical Academy, Kazan, Russia 420012*
[2]*Institute of Neuroscience, Newcastle University, UK*
[3]*Kazan Institute of Biochemistry and Biophysics, Kazan, Russia 420111*

Botulinum neurotoxin type A (BoNT/A) paralyses muscles by blocking acetylcholine (ACh) release from motor nerve terminals. Although highly toxic, it is used clinically to weaken muscles whose contraction is undesirable, as in dystonias. The effects of an injection of BoNT/A wear off after 3–4 months so repeated injections are often used. Recovery of neuromuscular transmission is accompanied by the formation of motor axon sprouts, some of which form new synaptic contacts. However, the functional importance of these new contacts is unknown. Using intracellular and focal extracellular recording we show that in the mouse epitrochleoanconeus (ETA), quantal release from the region of the original neuromuscular junction (NMJ) can be detected as soon as from new synaptic contacts, and generally accounts for $>$ 80% of total release. During recovery the synaptic delay and the rise and decay times of endplate potentials (EPPs) become prolonged approximately 3-fold, but return to normal after 2–3 months. When studied after 3–4 months, the response to repetitive stimulation at frequencies up to 100 Hz is normal. When two or three injections of BoNT/A are given at intervals of 3–4 months, quantal release returns to normal values more slowly than after a single injection (11 and 15 weeks to reach 50% of control values *versus* 6 weeks after a single injection). In addition, branching of the intramuscular muscular motor axons, the distribution of the NMJs and the structure of many individual NMJs remain abnormal. These findings highlight the plasticity of the mammalian NMJ but also suggest important limits to it.

(Received 5 March 2008; accepted after revision 7 May 2008; first published online 8 May 2008)
Corresponding author C. R. Slater: Institute of Neuroscience, Newcastle University, Framlington Place, Newcastle upon Tyne NE2 4HH, UK. Email: c.r.slater@ncl.ac.uk

Botulinum toxin A (BoNT/A) blocks signal transmission at the vertebrate neuromuscular junction (NMJ). Although highly toxic, it is used clinically in small doses which are injected intramuscularly to inhibit undesirable muscular contractions in various forms of dystonia and cerebral palsy and also cosmetically to reduce facial wrinkling. The blocking effect usually wears off after 3–4 months so repeated injections are required, sometimes over a period of years, to maintain the desired effect (Jankovic & Hallett, 1994; Dolly & Aoki, 2006). As many people are now being treated with BoNT/A, it is clearly important to understand both its short-, and long-term effects on muscle innervation.

BoNT/A is a metalloendoprotease. After binding to the synaptic vesicle protein SV2 at the surface of the motor nerve terminal (Dong *et al.* 2006), it is internalized and activated. It then specifically cleaves SNAP-25, an essential protein in exocytosis, thus preventing the 'quantal' release of ACh in response to nerve impulses (Schiavo *et al.* 2000). During the period of recovery from BoNT/A, sprouts grow out from the motor axon and may make contact with the muscle fibre (Duchen, 1970; Angaut-Petit *et al.* 1990; de Paiva *et al.* 1999; Santafe *et al.* 2000). Key synaptic proteins are subsequently expressed at many of these sites (Duchen, 1970; Yee & Pestronk, 1987; Juzans *et al.* 1996*b*; de Paiva *et al.* 1999). Although it is generally assumed that synaptic transmission occurs at these new contacts and mediates the initial functional recovery from BoNT/A (e.g. Molgo *et al.* 1990; Angaut-Petit *et al.* 1990) we are unaware that this view has ever been directly tested.

Some evidence concerning the role of new contacts in the recovery from BoNT/A comes from a study in which changes in the ability of identified NMJs to take up the membrane soluble fluorescent dye FM1-43 (Cochilla

 DOI: 10.1113/jphysiol.2008.153569

et al. 1999) were studied *in vivo* at various times after administering BoNT/A (de Paiva *et al.* 1999). Exposure to BoNT/A blocked activity-dependent FM1-43 labelling of the original nerve terminals within a few days. Newly formed axonal sprouts were seen to take up FM1-43 at a stage of recovery when uptake by the original terminal was still undetectable. However, 2–3 months after intoxication, the original terminal began to recover its ability to take up the dye and the sprouts were then withdrawn. These results were interpreted to mean that during the initial stage of recovery the sprouts, which appeared to be the only possible source of quantal ACh release, were exclusively responsible for the initial recovery of neuromuscular transmission.

The observations just described do not specifically demonstrate ACh release. Indeed, it is uncertain that the sensitivity of FM1-43 uptake experiments is adequate to detect the low levels of quantal release that may be able to excite muscle fibres that have been functionally denervated for some time. Using focal extracellular recording, capable of detecting the effects of a single ACh quantum with a spatial resolution of less than 10 μm (del Castillo & Katz, 1954), we have found that in the mouse ETA muscle (Bradley *et al.* 1989), although quantal release from the newly formed synaptic contacts does occur, substantially more quanta are released in the region of the original NMJ at all stages of recovery.

The action of BoNT/A is known to result in changes in the kinetics of quantal release at some synapses (Sakaba *et al.* 2005). In addition, there is evidence that types of voltage-gated calcium channel that are not normally expressed at mammalian NMJs are active during recovery from BoNT/A (Santafe *et al.* 2000). Although a number of previous studies have noted an increase in the incidence of 'slow' or 'giant' spontaneous mEPPs after exposure to BoNT/A (Thesleff *et al.* 1983; Kim *et al.* 1984), little has been reported about the properties of the evoked quantal release that account for functional recovery of the NMJ. We have therefore investigated changes in the temporal aspects of evoked ACh release and found that evoked responses are also significantly slower during the recovery from the effects of BoNT/A.

Although multiple injections of BoNT/A are widely used clinically to maintain muscle weakness, very little is known about the ability of the NMJ to recover from such repeated exposure. We have investigated the effects on NMJs in the mouse ETA of up to three injections, given at successive intervals of 3–4 months. Although there is substantial functional recovery even after three injections, this recovery is significantly slower than after a single injection and is associated with persisting structural abnormalities of the terminal and preterminal motor axon.

Preliminary accounts of some of our observations have been presented previously (Pang *et al.* 2002; Slater & Rogozhin, 2006).

Methods

BoNT/A Administration

All studies were authorized by Project Licence PPL 60/3024 issued by the UK Home Office and approved by the Newcastle University Ethics Committee. A total of 180 mice were used in the study.

All experiments were made on the epitrochleoanconeus muscle (ETA), located superficially on the medial aspect of the proximal forelimb (Bradley *et al.* 1989). To expose the muscle to BoNT/A, the mice were anaesthetized (3% isoflurane) and a small incision (1 mm) made in the skin in the right axilla. Ten microlitres of a solution containing 0.5 U of BoNT/A (BOTOX®, Allergan) in sterile saline was injected under the skin over the ETA using a 10 μl Hamilton syringe fitted with a 26 gauge needle. The skin was closed with a single suture and 0.2 ml Buprenorphine (1 : 100, subcutaneous) given to control pain. At the time of the acute experiment, the mice were killed by cervical dislocation.

Nerve–muscle preparations

In the adult mice used (female, *ca* 30 g) the ETA contains about 400 muscle fibres, each about 9 mm long with a mean diameter of about 35 μm. It is usually innervated by five to seven motor neurons contained in a small branch of the radial nerve. More than 90% of the muscle fibres are 'fast' as defined by myosin heavy chain immunolabelling.

The results from mice injected with BoNT/A were compared to those from uninjected mice, from mice injected with 10 μl of sterile saline (using the same injection procedure outlined above), or from the uninjected muscles contralateral to the experimental muscles.

The experiments reported here were made on mice of the strains CD1, MF1 or TO. No differences in the response to BoNT/A between the strains was noted.

Electrophysiological studies

Animals were killed at various times after BoNT/A injection by stunning and cervical dislocation. ETA nerve–muscle preparations were then dissected out and maintained at room temperature (20–23°C) in Liley's solution containing (mM): 137.8 NaCl, 4 KCl, 2 $CaCl_2$, 1 $MgCl_2$, 1 KH_2PO_4, 12 $NaHCO_3$, 11 glucose, gassed with 95% O_2–5% CO_2 (Liley, 1956). The preparations were pinned out in a recording chamber (Warner RC 27, Warner Instruments) with a volume of 2.5 ml, lined with Sylgard (Dow Corning). A continuous flow of gassed bathing fluid was maintained at 1 ml min^{-1} by a peristaltic pump. The muscle was viewed with a Leica DLFSA fluorescence microscope (Leica Microsystems) fitted with water immersion objectives (10–40×).

The nerve was drawn up into a suction electrode and routinely stimulated supramaximally with pulses of 0.1 ms duration. Intracellular recordings were made with glass electrodes (*ca* 10 MΩ resistance when filled with 3 M KCl), amplified by an Axoclamp 2B amplifier (Axon Instruments/Molecular Devices), further amplified and processed (filtered at 3 kHz) by a CyberAmp 380 (Axon Instruments), and digitized at a sampling rate of 41.6 kHz by a Digidata 1322A A/D converter (Axon Instruments) before being displayed and saved using pCLAMP 9 software (Axon Instruments). Extracellular signals were recorded with glass electrodes with an internal diameter of 2 μm, filled with bathing fluid, and were amplified by an AI402 head stage (Axon Instruments) feeding into the CyberAmp (filtered at 10 kHz) and digitized as above. Spontaneous events (mEPPs) were recorded in continuous samples of 1–2 min duration.

The preparations were initially viewed in bright field transmitted light with a 2.5× dry objective with a long working distance. Compound muscle action potentials (CMAPs) were recorded during stimulation of the nerve at 1 Hz to provide an indication of the overall state of functional innervation of the muscles before exposure to labelling and blocking reagents (see below) (Fig. 1). For this, an extracellular electrode (see above) was positioned approximately 100 μm above the surface of the muscle and moved parallel to the muscle fibres until a response was observed starting with an abrupt negative deflection, indicating proximity to the innervation zone. The electrode position was then further optimized by moving it laterally to the position where the largest response was observed.

Once CMAPs had been recorded, the motor axon terminals were labelled with the fluorescent dye 4-Di-2-ASP (Magrassi *et al.* 1987) (1 μM, 10 min; Molecular Probes/Invitrogen, Paisley, UK) and viewed with incident light using a fluorescein filter block (Leica I3). Neutral density filters were used to reduce the intensity of the incident light, typically 8-fold, to limit damage to the preparation from phototoxicity. Images of the labelled NMJs were recorded with a CoolSnapHQ cooled CCD camera (Photometrics), controlled by MetaMorph software (Molecular Devices). Exposures were usually of 1 s duration with the 40× objective.

Muscle action potentials were then blocked by exposing the muscles to μ-conotoxin GIIIB (μCTX, 2 μM; Peptide Institute, Osaka, Japan) for 15 min while the flow was stopped (Plomp *et al.* 1992). The toxin solution was then sucked out, the preparation returned to fresh bathing fluid and the flow resumed. This procedure blocked muscle contraction for 45–60 min, at which time the preparation was re-exposed to the toxin.

After blocking contraction with μCTX, one or two intracellular and two extracellular electrodes were positioned approximately and the objective changed to 40× water immersion (2 mm working distance) to search for NMJs located on the surface of the muscle. To record synaptic potentials, the intracellular electrodes were inserted into the muscle fibre 50–100 μm away from the NMJ, to minimize damage to the nerve terminal. When two intracellular electrodes were used, current was passed through one to maintain the membrane potential close to −75 mV. This ensured that measurements of the amplitude and time course of synaptic events, which are both influenced by the value of the membrane potential, were all made at nearly the same membrane potential. EPPs were routinely evoked by trains of 100 stimuli delivered at a frequency of 1 Hz. In some cases, described in the text, higher frequency trains were used. Spontaneous mEPPs were recorded during continuous records of 1 or 2 min duration. The EPPs and mEPPs recorded in this way are referred to below as EPP_{in} and $mEPP_{in}$ to distinguish them from events recorded with extracellular electrodes.

To make focal recordings of synaptic events (del Castillo & Katz, 1956) an extracellular electrode was positioned close to a site of interest along the axon terminal or a sprout. Gentle pressure was then applied, under visual control, to bring the electrode into contact with the axon without causing damage (signalled by an abrupt increase in mEPP frequency).

The response to nerve stimulation recorded from a single extracellular electrode positioned near the innervation zone in a muscle blocked with μCTX is the sum of a diffuse field potential from the summed EPPs at a large number of NMJs, analogous to the CMAP, and a much more localized response from the site of interest, which we refer to here as EPP_{ex}. The field response varied little with movements of the electrode of even 100 s of μm, but the local response was very sensitive to movements of a few micrometres. To obtain the local response without 'contamination' by the field response, a second extracellular electrode was frequently positioned 5–10 μm away from the site of focal recording and the signal from this reference electrode was subtracted from the signal from the focal electrode (Katz & Miledi, 1965). Successful placement of the focal electrode on the nerve was indicated by the presence of a nerve action potential in the average of a set of 25–100 responses (Angaut-Petit *et al.* 1990).

In muscles that had been treated with BoNT/A, the structure of the original NMJs was sometimes so altered that they could not be identified with certainty. However, fibres with clearly identifiable original NMJs were used when possible, to allow reliable comparison of events associated with the new sprouts with those arising in the region of the original NMJs. In these muscles, most recordings from sprouts were made within 50 μm of the original NMJs.

Analysis of electrophysiological data

All electrophysiological recordings were analysed with the Clampfit package in pCLAMP 9 (Axon Instruments). Spontaneous events were extracted using the 'template search' facility.

Kinetics of synaptic events. EPP_{ex} latency was defined as the time from the onset of the stimulus artefact to the time when the potential reached 20% of its peak value. The rise time and decay time of synaptic events was defined as the time taken to go from 10 to 90%, or 90–10%, respectively, of the peak amplitude.

Quantal content. The quantal content of the EPP_{in} was estimated from the ratio of EPP_{in} amplitude to $mEPP_{in}$ amplitude, after suitable correction of the signals for membrane potential and nonlinear summation, assuming a reversal potential of 0 mV (Martin, 1955; Slater *et al.* 1992). No additional adjustment was made for the effect of membrane capacity on quantal content (McLachlan & Martin, 1981) (equivalent to setting their $f = 1$).

Immunolabelling

Whole ETA muscles were incubated in rhodamine–α-bungarotoxin (R-BgTx, 10^{-6} M; Molecular Probes/Invitrogen) in Liley's solution for 1 h and then washed thoroughly. They were then fixed in 0.5–1% paraformaldehyde in 0.1 M phosphate buffer for 30 min. After washing in buffer, muscles were permeabilized in alcohols (ethanol for 10 min followed by methanol for 10 min, both at -20°C) followed by incubation in Triton X-100 (0.1%, 10 min, room temperature). They were then incubated overnight at 4°C in a mixture of rabbit anti-neurofilament protein (NFP; AB1982, Chemicon) and rabbit anti-synaptophysin (RB1461, Neomarkers, Stratech), each at a dilution of 1/100, in PBS containing 3% BSA (Sigma-Aldrich) and 0.1 M lysine (Sigma-Aldrich). The next day, after washing in PBS, they were incubated for 3 h at room temperature in FITC–swine anti-rabbit (1/100) (DAKO) which had been preincubated in half the volume of neat rat serum to reduce non-specific binding. After washing overnight in PBS, the muscles were mounted on slides in Vectashield (Vector Laboratories).

Labelling of single teased muscle fibres

To assess the distribution of differentiated postsynaptic sites, muscles were labelled with R-BgTx (10^{-6} M, 1 h) and then fixed in 1% paraformaldehyde 1 h, 0.1 M phosphate buffer. After fixation junctional regions, several millimetres long, of 30–50 individual fibres from each muscle studied were dissected out and mounted in Vectashield for subsequent analysis.

Microscopy

Image recording. Fixed preparations and teased fibres were viewed with a Leica DMRA fluorescence microscope (Leica Microsystems) using filter blocks N21 (TMRITC) and L5 (FITC, selective). Images were captured with a SPOT-II camera (Diagnostics Instruments) under control by MetaMorph. When appropriate, Z-series were recorded at a spacing of 1 or 2 μm using a 50$\times$ oil immersion objective.

Image analysis. The area and number of regions of postsynaptic differentiation were determined from teased fibres. For each fibre, each of what appeared to be separate regions of high R-BgTx labelling was outlined by hand. The regions of high R-BgTx labelling at what appeared to be the original endplate, i.e. to consist of a closely packed cluster of highly intense spots, were also outlined. The areas of all regions were calculated using MetaMorph.

Statistical analysis and data presentation

Averaged data are presented with the S.D. and relevant sample size. The significance of differences between means was determined using Student's two-sided paired *t* test, accounting for small samples where appropriate. The relationship between number of BoNT/A injections and rate of functional recovery, illustrated in Fig. 12, was investigated using analysis of covariance (http://udel.edu/∼mcdonanld/statancova.html).

Results

The initial aim of this study was to assess the contribution of new synaptic contacts to the functional recovery of mouse NMJs after exposure to BoNT/A. Before doing this, it was necessary to establish the time course of functional recovery and axonal sprout outgrowth as it occurs in the mouse ETA muscle, since this has not been previously described.

Time course of recovery from a single injection of BoNT/A

Neuromuscular transmission. Nerve-evoked contraction of the ETA was fully blocked within 1–2 days of BoNT/A injection. The first visible signs of recovery occurred 2–3 weeks later, when weak contractions in response to nerve stimulation could be seen. During the next 3–4 weeks the contractions grew in strength and became hard to distinguish from normal by eye. During the period of impaired transmission, many muscles displayed spontaneous fibrillation, in a manner typical of denervated muscles. This was most prominent 1–4 weeks after

BoNT/A treatment. Occasionally spontaneous contractions were seen up to 4 months after BoNT/A treatment but not after that time.

To provide a more quantitative measure of the overall recovery of function, compound muscle action potentials (CMAPs) were recorded (Fig. 1*A*). In control ETA muscles these have a mean amplitude of 1.92 mV (S.D. 0.48 mV, $n = 10$). They were completely abolished within 1–2 days after BoNT/A injection (Fig. 1*B*). During recovery, CMAPs were first detected at 2–3 weeks, and some were within the normal range of amplitudes 8–10 weeks after BoNT/A injection. Nonetheless, the CMAP amplitude was usually less than normal even 10–12 weeks after BoNT/A.

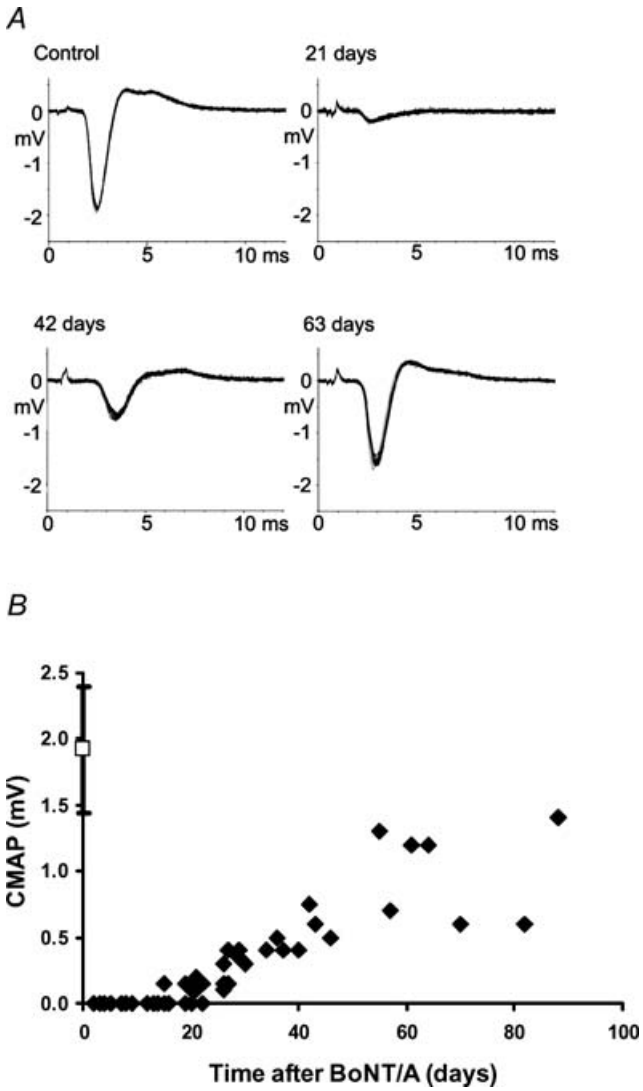

Figure 1. Recovery of CMAP after exposure of mouse ETA to BoNT/A
A, recordings of CMAPs at representative times during the course of recovery. *B*, changes in amplitude of negative peak of CMAP as a function of time after exposure to BoNT/A. Each point represents a single muscle. Open symbol on ordinate shows mean value for 10 control muscles ± S.D.

To assess the changes in quantal release of ACh from the whole motor nerve terminal we used intracellular electrodes to record EPP_{in}s and $mEPP_{in}$s. From their amplitudes we calculated the quantal content (see Methods). These values are shown, as a function of time after BoNT/A injection, in Fig. 2. At NMJs in normal ETA muscles, the quantal content in our conditions was 57.9 (S.D. 26.8, $n = 10$). The quantal content fell to < 0.1 within 1–2 days after BoNT/A. The first NMJs where the QC had increased to > 1 were seen 12 days after injecting BoNT/A. By 6–7 weeks after BoNT/A the QC was about 60% (33.2, S.D. 13.1, $n = 3$) of normal and after 10–14 weeks was indistinguishable from normal (61.6, S.D. 15.2, $n = 5$). The mean EPP_{in} amplitude was significantly correlated with the CMAP amplitude in the same muscle throughout the recovery period ($r = 0.92$, $n = 53$, $P < 0.001$). This implies that the experimental treatments used to record EPPs (μCTX, 4-Di-2-ASP) did not have a disproportionate effect on, for example, quantal release early in recovery. Mice of several strains were used in the course of this project (see Methods). No differences between the strains were observed in either the timing or extent of recovery.

Nerve sprouting and AChR accumulation. After exposure to a blocking dose of BoNT/A, sprouts grow out from the motor axon terminals and appear to establish new synaptic contacts with nearby muscle fibres (Duchen, 1970; Juzans *et al.* 1996*a*; de Paiva *et al.* 1999; Santafe *et al.* 2000). We investigated the process of axonal sprout formation and differentiation to see how it was related in time to the recovery of quantal release in the ETA. Muscles were labelled with antibodies to NFP and synaptophysin to reveal the nerves and their terminals and with R-BgTx to visualize the distribution of postsynaptic AChRs.

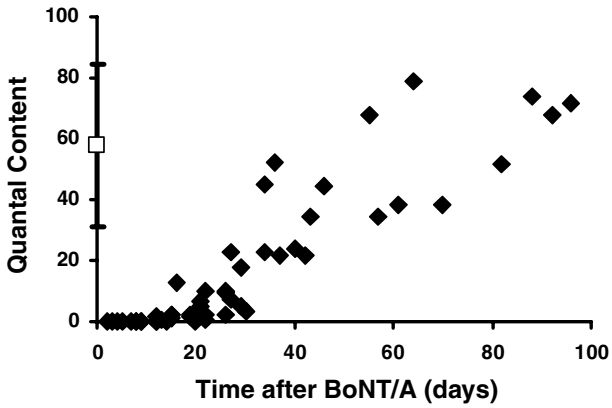

Figure 2. Recovery of evoked quantal release after exposure of mouse ETA to BoNT/A
Quantal content of the EPP_{in}, calculated from mean amplitudes of $mEPP_{in}$s and EPP_{in}s (see Methods). Each point represents the mean of values from approximately 10 NMJs in a single muscle. Open symbol on ordinate shows mean value for 10 control muscles ± S.D.

Axonal sprouts could be seen extending from the motor axon terminals within a week or less of BoNT/A injection (Fig. 3*A*, '1–2 weeks'). Over the next few weeks, these sprouts grew further, primarily along the muscle fibres. From about 2 weeks after BoNT/A injection, lateral branches began to emerge from the main longitudinal sprouts and then gradually increased in length. From an early stage, many of the growing ends of the sprouts ended in roughly circular varicosities, typically about 3 μm in diameter.

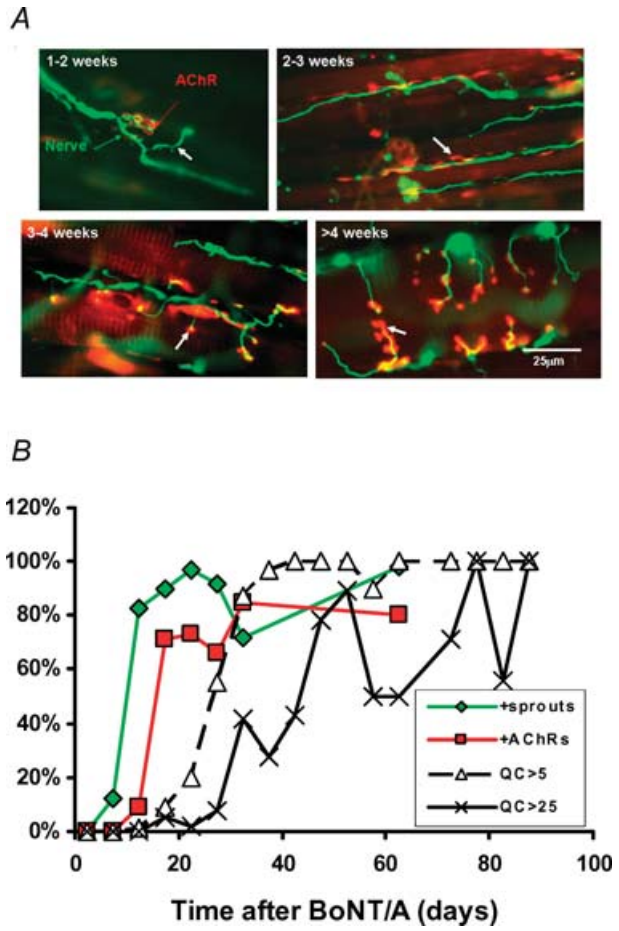

Figure 3. Axonal sprouting induced by exposure of mouse ETA muscle to BoNT/A
A, images of terminal motor innervation at representative times during recovery. Nerves labelled with antibodies to neurofilament protein and synaptophysin (green), AChRs in muscle labelled with R-BgTx (red). The appearances illustrated in each panel are typical of those seen at the indicated times after injection of BoNT/A. *B*, time course of events in the response of NMJs to exposure to BoNT/A, expressed as the fraction of NMJs (%) having the features shown. Sprouts form within the first week or so and AChR clusters appear a few days later. The increase in quantal release is indicated by curves showing the fraction of NMJs with QC > 5, representing an unambiguous increase from the blocked level, and of NMJs with QC > 25, a value likely to cause muscle fibre excitation and contraction. Each point represents the mean of values from 1–5 muscles.

Clusters of AChRs, adjacent to the growing sprouts, were apparent from about 2 weeks of BoNT/A injection (Fig. 3*A*, '2–3 weeks'). Initially, these appeared as faint, poorly defined clusters lying along the sprouts. As the lateral branches formed, most of the AChR clusters took on a circular, spot-like form, coincident with the varicosities, and grew brighter and more clearly defined (Fig. 3*A*, '3–4 weeks'). At times greater than 4 weeks after BoNT/A injection many of the AChR clusters had bright rims, similar to those seen at normal NMJs, suggesting the presence of a concave depression in the surface of the muscle fibre at the new synaptic sites (Fig. 3*A*, '> 4 weeks'). At no time in the formation and maturation of new contacts were AChR clusters seen that were not close to axon sprouts.

We quantified the incidence of sprouts and AChR clusters after BoNT/A intoxication in order to relate their appearance to the onset of evoked quantal release (Fig. 3*B*). At a population level, the AChR clusters form about 5 days after the formation of sprouts. A clear increase in quantal content, represented by the fraction of NMJs where the quantal content has increased to > 5 (normal value 58), is present at 50% of NMJs by about a week after AChR clusters form. To trigger a muscle action potential and contraction probably requires the release of about 25 quanta (based on data from rat soleus muscles; Wood & Slater, 1997). As shown in Fig. 3*B*, this level of release occurs at 50% of NMJs by about 40 days after BoNT/A.

In summary, our observations of the ETA confirm earlier observations (de Paiva *et al.* 1999) that after an injection of BoNT/A, well formed axonal sprouts whose terminals are associated with AChR clusters are already present for several days before quantal release of ACh becomes readily detectable. However, the entire recovery process occurs more rapidly in ETA than in the mouse soleus, extensor digitorum longus or levator auris (LAL) (Duchen, 1970; Tonge, 1974; Santafe *et al.* 2000). We have confirmed the slower recovery in soleus (L. Gurney, K. K. Pang & C. R. Slater, unpublished observations).

How much do new synaptic contacts contribute to functional recovery?

To estimate the contribution of new synaptic sites to the initial recovery after exposure to BoNT/A, we first located individual new synaptic sites and then estimated the intensity of release from them. We then determined the extent and number of such new synaptic contacts. Finally we used these data to estimate the summed contribution of release from all the new sites on a muscle fibre to the total quantal content.

Location of release sites. The spatial resolution of intracellular recording does not allow quanta released from new synaptic sites to be easily distinguished from those

released from the site of the original NMJ. To study release from new sprouts, we therefore used focal extracellular recording (del Castillo & Katz, 1954), which allows the sites of synaptic current generation to be defined with a resolution of 5–10 μm.

The nerve–muscle preparations were routinely labelled with the mitochondrial dye 4-Di-2-ASP to allow the nerve and its sprouts to be visualized during electrophysiological recording (Magrassi *et al.* 1987). Normal nerve terminals labelled with this dye generally appear as a compact cluster of discrete varicosities, each typically 2–3 μm in diameter (Fig. 4). Extracellular electrodes placed near such labelled spots frequently record both spontaneous and evoked quantal events which we refer to as EPP_{ex}. Comparison of records from two electrodes placed at different spots at the same normal NMJ confirms that this mode of recording can differentiate between quanta released from sites less than 10 μm apart (Fig. 4).

Axonal sprouts induced by BoNT/A are also labelled by 4-Di-2-ASP (Fig. 5*A*) (cf. de Paiva *et al.* 1999). Like normal nerve terminals they appear as a number of discrete varicosities, but ones that lie outside a region bounded by a smoothly contoured line enclosing the original nerve terminal. Such a line is shown in Fig. 5*A*. In the later stages of recovery from BoNT/A, recordings of evoked and spontaneous quantal release could almost always be obtained when the electrode was placed over such spots (see below), confirming that they correspond to discrete sites of quantal release along the sprouts. Movements of the electrode of only a few micrometres away from these spots resulted in a great reduction in the amplitude of the spontaneous events. At the same time, the amplitude of the evoked responses was reduced to a level that was relatively independent of position. This 'field' signal, analogous to the CMAP, represents the effects of the summed end-plate currents from many NMJs. We often placed a second extracellular electrode near the first to record this 'field' EPP so that it could be subtracted to reveal the 'specific', position-dependent responses (cf. Fig. 5*B*) (Katz & Miledi, 1965).

During the initial recovery phase, 2–6 weeks after BoNT/A, synaptic events could be recorded with an extracellular electrode both at the sites of the original NMJs and at varicosities on sprouts (Fig. 5*B*). In this figure, the six to eight responses shown were selected from series of 100 trials to illustrate the range of amplitudes, and do not necessarily represent the average responses (see below). In general, synaptic activity was always easier to record from the original NMJs than from the sprouts. However, this effect is difficult to quantify because at many spots it was necessary to reposition the recording electrode repeatedly before synaptic events were detected. Thus the absence of detectable events at any particular recording site was not always a good indication of an absence of quantal release. On the other hand, even a single recorded event, as illustrated in Fig. 5*B* 'New', is clear evidence that the electrode is adequately placed to record synaptic events.

An important additional indication that the recording electrode was placed over a sprout was the ability to record an extracellular nerve action potential (Brigant & Mallart, 1982; Mallart & Brigant, 1982; Angaut-Petit *et al.* 1990). The detection of these signals was improved if the electrode was pressed against the sprout. However, this risked causing mechanical damage. We therefore generally looked for the nerve action potentials in averages of 25–100 traces. Only when both 4-Di-2-ASP labelling and an extracellular nerve action potential were present was the absence of detectable synaptic events taken as a significant negative finding.

Assessment of release. Early in recovery only occasional stimuli evoked detectable responses at any extracellular recording site (Fig. 5*B*). For example, at the NMJ illustrated

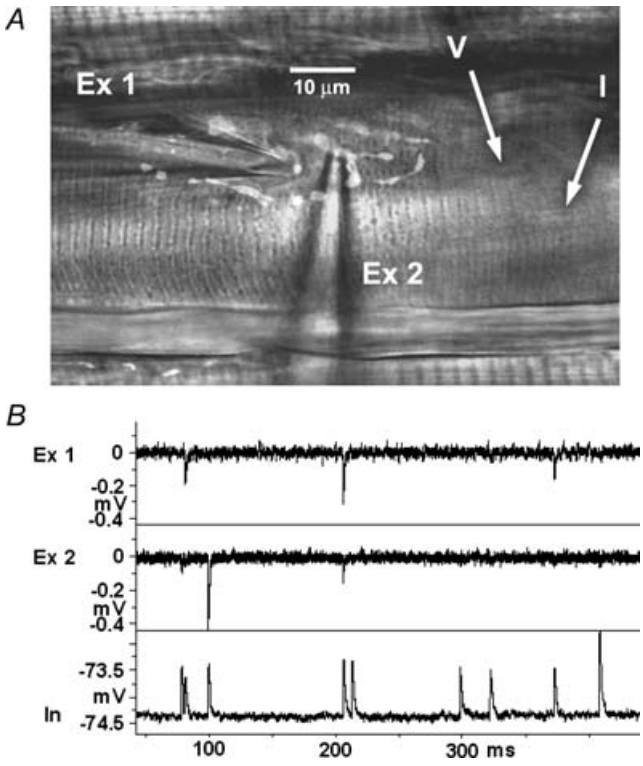

Figure 4. Spatial discrimination of focal extracellular recording
A, a fluorescence image of an ETA NMJ after labelling with 4-Di-2-ASP merged with a bright field image showing muscle fibre and electrodes. Two extracellular electrodes ('Ex 1' and 'Ex 2') are positioned on different parts of the nerve terminal, 8.9 μm apart. The position of the two intracellular electrodes ('V' and 'I'), both slightly out of focus in this image, are indicated by arrows. Electrode 'V' is used to record membrane potential and electrode 'I' is used to pass current to maintain membrane potential near −75 mV. *B*, the bottom trace shows mEPPs recorded with the intracellular electrode ('V') and the other two traces show recordings by the two extracellular electrodes. The difference in the recordings from these two electrodes gives an indication of the spatial resolution of this approach.

in Fig. 5, 21 days after BoNT/A, responses from the original NMJ were seen in 28/100 trials and in only 1/100 trials at the 'new' site. In contrast, EPP_{in}s were recorded in 82/100 and 84/100 in these two series of trials.

The very low frequency of spontaneous $mEPP_{ex}$s observed made it impractical to estimate directly the mean number of quanta released by a single nerve impulse from new synaptic spots. Instead, we made the assumption that during the early stages of recovery, as in many other situations where quantal content is low, the release process obeyed Poisson statistics (Katz, 1969). Analysis of the distribution of amplitudes of EPP_{ex}s suggested that this was a valid assumption. For example, at the NMJ illustrated in Fig. 5, the series of 100 trials recorded from the 'original' site included 72 'failures', i.e. stimuli that failed to evoke a detectable response, 24 responses whose amplitude was intermediate in amplitude (mean 0.15 ± 0.024 mV) and four responses whose amplitude was clearly greater (mean 0.27 ± 0.030 mV). The Poisson distribution predicts that for a failure rate of 72%, 24% of the responses should consist of 1 quantum and 4% of 2. In this case, the observed distribution of EPP_{ex} amplitudes agreed well with that predicted by the Poisson distribution for a mean quantal content of 0.33.

We therefore used the fraction of response 'failures' to estimate the mean number of quanta released in the pickup area of the electrode. We defined this value as the 'local' quantal content (QC_{local}), i.e. the mean number of quanta detected by the extracellular electrode at a given recording site in response to a single stimulus. An inherent limitation of this method for estimating QC_{local} is that it can only be used when the fraction of failures is greater than about 5%. This was generally the case up to 6–8 weeks after exposure to BoNT/A.

Comparison of the QC_{local} at original and new synaptic sites shows that at the earliest stages of functional recovery, 2–3 weeks after exposure to BoNT/A, more quanta were released by a single nerve action potential at recording sites at the original NMJ than at the new synaptic spots (Fig. 6). This situation was maintained for at least 2 months, by which time overall recovery of quantal release was more than 50% complete. During the period 2–12 weeks after exposure to BoNT/A, the mean QC_{local} at 'new' synaptic spots was 17% (s.d. 19%, $n = 10$ muscles) of that from sites in the original junctional region.

Extent of new synaptic contacts. To estimate the summed contribution of quantal release from new synaptic contacts to the overall quantal content at recovering NMJs, we needed to establish the spatial extent and number of the new synaptic regions. To do this we defined and measured all the regions of high AChR density, marked by labelling with R-BgTx, on individual ETA muscle fibres teased from muscles at various times after exposure to BoNT/A. Examples of muscle fibres in different stages of recovery are shown in Fig. 7*A*. In the example from 14 days, when most NMJs have many axonal sprouts, no new AChR clusters have formed. In the example from 17 days, faint, poorly defined clusters can be seen up to 75 μm from the original NMJ. By 24 days, the AChR clusters are much brighter

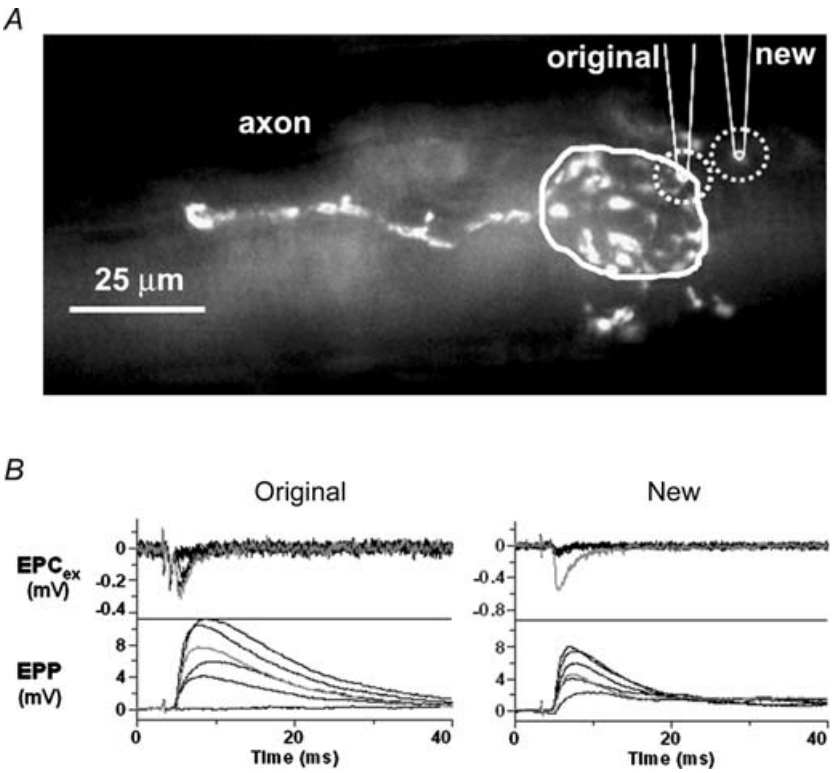

Figure 5. Localization of evoked quantal release
A, image of nerve terminal, labelled with 4-Di-2-ASP, from mouse ETA 21 days after exposure to BoNT/A. Two extracellular recording positions are indicated, one over part of the original terminal and one over a newly formed synaptic spot about 10 μm away. The limits of what is considered the original terminal are shown by a continuous white line. *B*, recordings from the two sites depicted in *A*. For each site the upper traces are from the extracellular electrode, with downward deflections indicating evoked synaptic currents. The lower traces are from an intracellular electrode. Six pairs of traces, which were selected from a series of 100 to show the range of values observed, are shown for each site. One pair from each site has been shown in grey. At each site most stimuli failed to evoke any localized extracellular response even though an EPP_{in} was present. At the 'new' site the trace in grey was the only clear response seen in 100 trials. Further details in text.

and are more clearly defined. We traced around each of these AChR clusters and then measured its area. Most individual AChR 'spots' are 3–5 μm in diameter. Often, a number of spots were close enough to each other so that their boundaries were hard to resolve. In these cases, we traced around a cluster of contiguous spots. We refer below to a 'region' of high AChR density as a spot or a collection of spots so close together that they were included in the same measuring profile.

The total area of new synaptic contacts on a given fibre was generally substantially less than that of the original NMJ (Fig. 7*B*). During the first 3 weeks after BoNT/A injection, the total area of new contacts per muscle fibre increased to about 70 μm^2 and then remained at that level (mean 67.5 μm^2, S.D. 33.6, $n = 15$ muscles, for the period 3–7 weeks). In contrast, original NMJs have an area of 218 μm^2 (S.D. 35.0, $n = 15$). Thus, during most of the recovery phase, the area of the new contacts was about 30% of that of the originals, or about 25% of the total area of high AChR density per muscle fibre. The mean number of contiguous regions of AChR labelling during the period 3–7 weeks after BoNT/A was 4.95 (S.D. 2.05, $n = 8$ muscles) per muscle fibre (Fig. 7*C*), giving an average area of such regions as 13.6 μm^2. This analysis shows that in the majority of muscle fibres, the area of new synaptic contacts remained a relatively small fraction of the total synaptic area.

Contribution of new synaptic contacts to functional recovery. We estimated the quantal content from new contacts by assuming that our extracellular recordings detected quanta from a single region of new synaptic contact. This seemed justified because the average area of these regions (13.6 μm^2) is well within the pickup area of the extracellular electrodes (100–300 μm^2), and there was generally a distance of at least 10 μm between these regions (cf. Fig. 7*A*; 17 and 24 days). On this basis, the total quantal content is given by the product of the number of regions per muscle fibre and the local quantal content. When new AChR clusters were closer together than 10 μm, this procedure would tend to overestimate release from new spots. The resulting values are shown in Fig. 8, in which data have been pooled into bins 5 days wide.

From the earliest time when recovery of quantal release can be reliably detected, the total number of quanta released from new synaptic contacts is substantially less than from the sites of the original NMJs. On average, throughout the first 6 weeks after BoNT/A, release from new contacts was 17% of that from original NMJs (S.D. 19%, $n = 10$).

Temporal features of evoked synaptic events during recovery

In the course of our studies it became clear that there were significant changes in both the latency and time course of the evoked synaptic responses at NMJs during the process of recovery from BoNT/A. Since it is known that cleavage of SNAP-25 by BoNT/A influences the dynamics of quantal release at other synapses (Sakaba *et al.* 2005), we attempted to define these changes in more detail.

Latency and synaptic delay of evoked synaptic events during recovery from BoNT/A. In a previous study, made on the LAL muscle of mice, it was found that the latency of EPPs increased during recovery from BoNT/A (Santafe *et al.* 2000). The latency of the EPP has two components: the conduction time in the nerve and the synaptic delay between the arrival of the nerve impulse and detectable quantal release. To distinguish between these factors as determinants of the increased latency, we studied EPP_{ex}s. During the first 30 days after BoNT/A, the average latency from stimulus to onset of EPP_{ex} was nearly twice as long as normal (control, 1.1 ± 0.13 ms, $n = 5$ *versus* BoNT/A, 1.9 ± 0.33 ms, $n = 23$, $P < 0.0001$) (Fig. 9*A* and *B*).

The conduction velocity along sprouts evoked by BoNT/A in the mouse LAL has been reported as 0.24 m s^{-1} (Angaut-Petit *et al.* 1990), a value not far from that originally measured at normal frog motor nerve terminals (0.3 m s^{-1}) (Katz & Miledi, 1965). In the ETA, in muscles up to 36 days after BoNT/A, we observed a value of 0.17 m s^{-1} (S.D. 0.08, $n = 8$). Few of the sprouts we studied were more than 100 μm long (see Santafe *et al.* 2000). For a sprout of that length, assuming a conduction

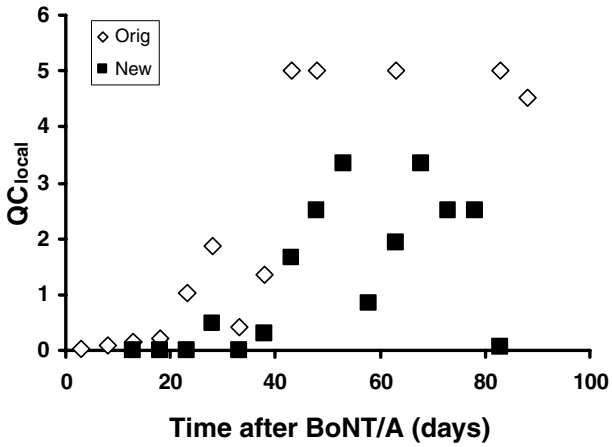

Figure 6. Comparison of the intensity of evoked quantal release at new and original synaptic sites during recovery of mouse ETA NMJs from exposure to BoNT/A
The local quantal contents (QC_{local}) of the extracellular responses to nerve stimulation, calculated from the fraction of 'failures' using the Poisson distribution (see text for further details), are shown as a function of time after exposure to BoNT/A. Each point represents the mean of values from 1 to 27 (mean 18) fibres in 2–8 (mean 5) muscles at times < 40 days, and 1–2 muscles for times > 40 days, pooled into 5-day intervals after exposure to BoNT/A.

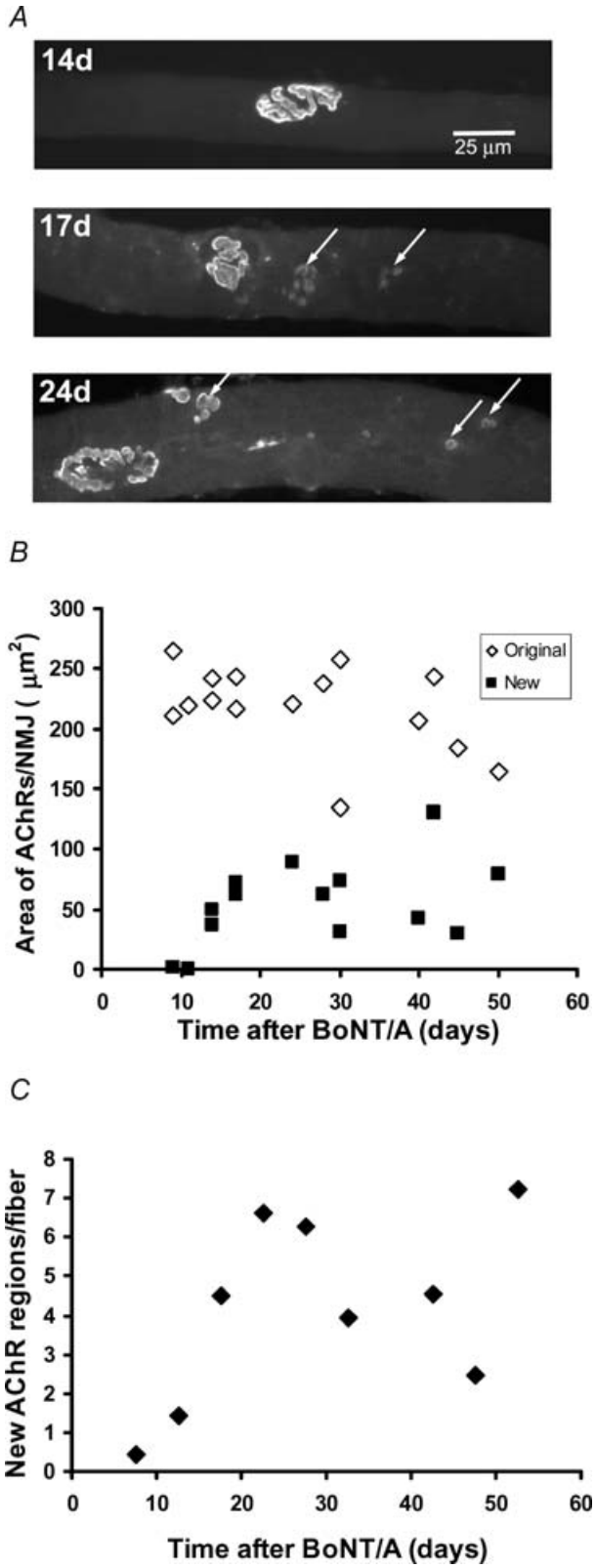

Figure 7. Extent of AChR clusters at new synaptic spots that form during recovery of mouse ETA muscles after exposure to BoNT/A

A, images of AChRs, labelled with R-BgTx, at representative times during recovery. Arrows point to new synaptic spots. At 17 days these are fainter and less well-defined than at 24 days. *B*, total area, per muscle fibre, of AChR clusters at original NMJs and at new synaptic sites as a function of time after exposure to BoNT/A. At all times the area of new sites is substantially less than that of the original NMJs. *C*, mean number of separate regions of high AChR density on individual muscle fibres as a function of time after exposure to BoNT/A. Each point represents the mean of data from 1 to 4 muscles pooled into 5-day intervals after exposure to BoNT/A.

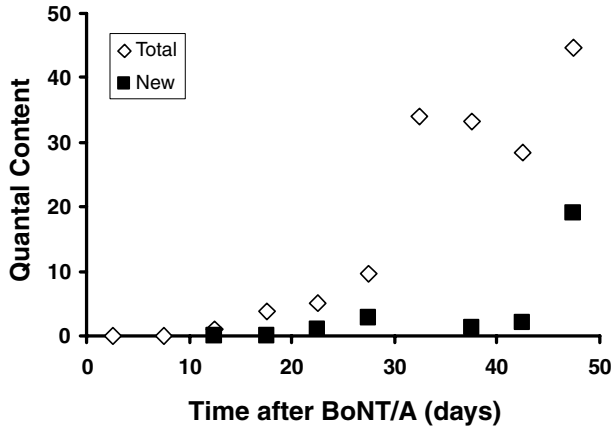

Figure 8. Estimated contribution of quantal release from new synaptic spots to neuromuscular transmission during recovery from exposure of mouse ETA to BoNT/A

Open symbols, total quantal content recorded with an intracellular electrode; filled symbols, estimated quantal release from all new synaptic spots on individual muscle fibres (see text). Points represent mean values from 1 to 8 (mean 3.4) muscles, pooled into 5-day intervals after exposure to BoNT/A. Typically 2–3 fibres were studied in detail in each muscle. Note that at all times, the estimated contribution from new synaptic sites is a small fraction of the total.

velocity of 0.2 m s^{-1}, the conduction time along the entire sprout would be 0.5 ms. While it is thus likely that the conduction time accounts for some of the increased latency at new synaptic sites on the longest sprouts, we observed no significant difference between the observed average latencies at sites on sprouts (1.9 ± 0.48 ms, $n = 5$) and at the site of the original NMJ (1.9 ± 0.26 ms, $n = 18$) during the period up to 30 days after exposure to BoNT/A.

In contrast, we found clear evidence for an increase in the second component of EPP latency, the synaptic delay. We defined this as the time from the negative peak of the nerve action potential to the foot of the EPP_{ex} (Fig. 9*C*). At those NMJs where both a clear nerve action potential and EPP_{ex} were recorded, the synaptic delay increased from a normal value of 0.32 ± 0.034 ms ($n = 8$) to 0.73 ± 0.16 ms ($n = 26$ NMJs studied up to 30 days after exposure to BoNT/A, $P < 0.0001$). There was no significant difference between the delays observed at new and original sites (0.70 ± 0.14 ms, $n = 6$ *versus* 0.74 ± 0.17 ms, $n = 20$). Thus, during recovery from BoNT/A, the events coupling

nerve terminal depolarization to quantal release occur more slowly than normal.

Kinetics of synaptic potentials during recovery. During the early stages of recovery of transmission, evoked synaptic potentials with an unusually slow time course were sometimes seen (Fig. 10). Some of these recalled the 'giant' or 'slow' spontaneous miniature potentials previously described by others (Thesleff & Molgo, 1983; Thesleff *et al.* 1983; Kim *et al.* 1984). In those earlier studies, changes in the time course of evoked events were not reported.

A systematic study of the time course of individual EPP_{in}s showed that during the initial recovery process, both the rise and decay times were substantially longer than normal (Fig. 10*A* and *B*). In the period 12–22 days after exposure to BoNT/A, the rise time of EPP_{in}s was 1.61 ± 0.20 ms (control 0.53 ± 0.015 ms, $P = 0.0014$) and the decay time was 15.07 ± 1.87 ms (control 4.52 ± 1.19 ms, $P = 0.0002$). The mean values for individual muscles were highly significantly correlated ($P < 0.001$). The period of prolonged kinetics lasted about 4 weeks, and was followed by a return to normal values about 6 weeks after exposure to BoNT/A (Fig. 10*C* and *D*). Thus, the average kinetic properties of the EPP_{in}s returned to near normal values when the mean quantal content was about 25, still less than half its normal value. This suggests that the changes in EPP_{in} time course at individual synaptic sites are short-lived.

Of particular interest were a small number of fibres where more than one population of EPP_{in}s, differing in time course were present (Fig. 10*E*–*H*). Figure 10*E* shows most of the 71 events evoked during a series of 100 trials from one of these fibres. Of the 100 responses, 29 were 'failures', indicating that the quantal content of the EPP_{in} was 1.24. Of the events that were evoked, 52 were 'pure fast' (e.g. Fig. 10*F*), 7 were 'pure slow' (Fig. 10*H*) and 12 were 'mixed' (Fig. 10*G*), apparently the sum of a fast and a slow response. Thus 64 responses included a fast response and 19 a slow response. If the responses of these two classes arose independently, the probability that both a fast and a slow response would appear in the same trial is $0.64 \times 0.19 = 0.12$. This predicts that 12 responses should be mixed, whereas 11 were observed. The results of this analysis thus support the view that the two classes of response at this and several other similar NMJs were evoked independently. Unfortunately, these fibres were too rare to allow detailed analysis of the sites of origin of the two different classes of evoked response.

Response to repetitive stimulation. The results described so far relate to NMJs stimulated at 1 Hz. As a further test of the recovery of quantal release, in conditions more related to normal functioning, we studied the response

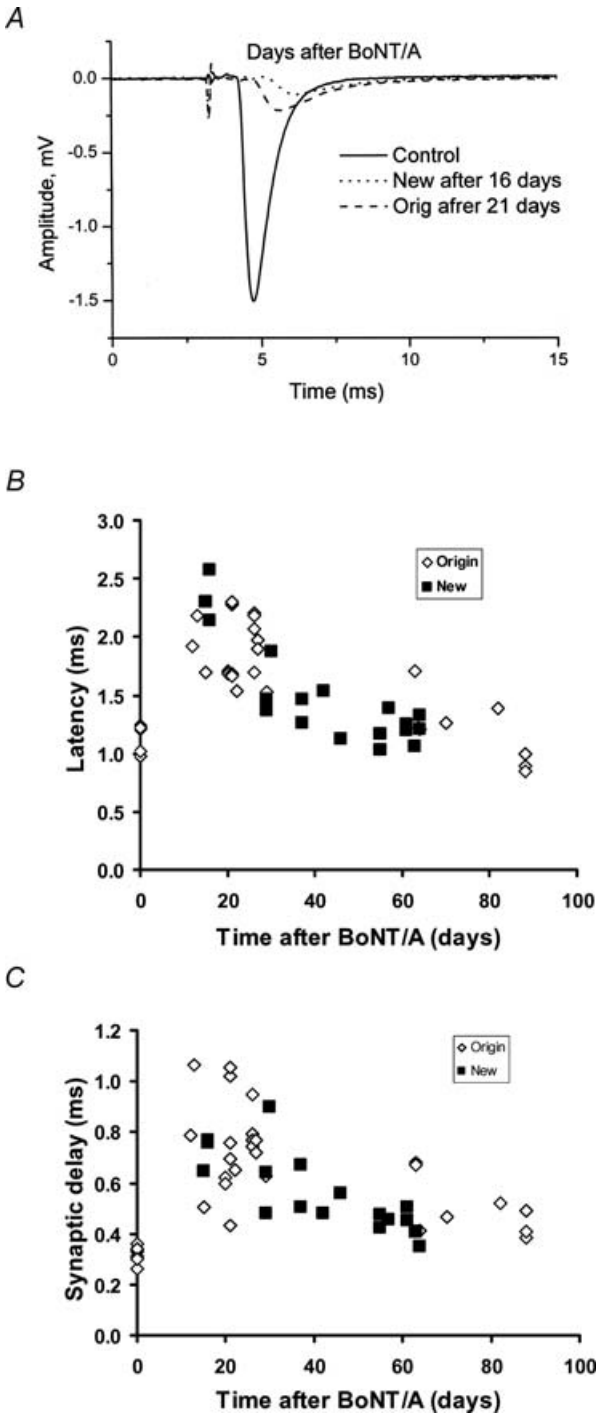

Figure 9. Temporal changes in onset of evoked responses during recovery from BoNT/A
A, records showing averaged EPP_{ex}s recorded from a control NMJ, from new synaptic contacts 16 days after exposure to BoNT/A and from the site of an original NMJs 21 days after exposure to BoNT/A. *B*, changes in EPP_{ex} latency (time from stimulus artefact to 20% of peak amplitude of EPP). *C*, changes in synaptic delay (time from negative peak of nerve action potential to 20% of peak amplitude of EPP_{ex}). Note that the time course with which both latency and synaptic delay approach normal values is similar at the new contacts and at the original NMJs. Each data point represents averaged data from one recording site.

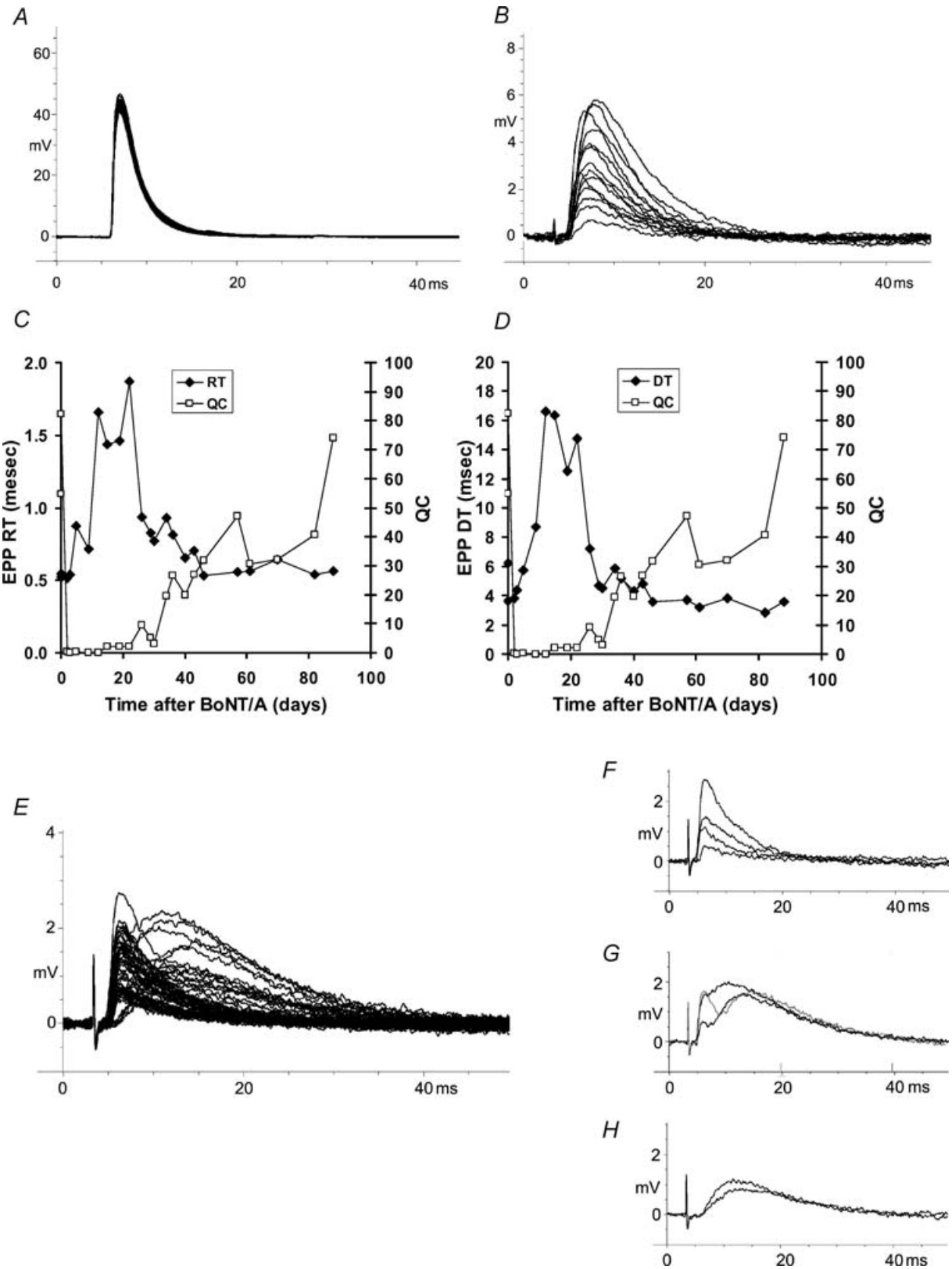

Figure 10. Changes in kinetic properties of EPP_{in}s during recovery from exposure of mouse ETA muscles to BoNT/A

All recordings show EPP_{in}s selected from trains of 100 stimuli (1 Hz). *A*, typical EPPs (14 superimposed) from uninjected muscles. Note minimal variation of amplitude or time course. *B*, superimposed EPP_{in}s from ETA injected

to repetitive stimulation in some muscles 4 months after exposure to BoNT/A. Over the frequency range of 1–100 Hz, the properties of release at NMJs exposed to a single injection at BoNT/A were qualitatively similar to normal (Fig. 11). At frequencies below 50 Hz there was a depression of release during a train of 100 stimuli. This included both a rapid phase consisting of the first 20 or so responses followed by a much slower phase. At 50 and 100 Hz, these two phases of depression were preceded by a brief phase of potentiation. This resulted in EPP_{in}s amplitudes about 1.2 times the initial value at both treated and control NMJs.

Recovery from multiple injections of BoNT/A

Recovery of neuromuscular transmission. It is clear from clinical experience that some degree of functional recovery is possible even after multiple injections of BoNT/A. However, we are unaware of any reports of systematic studies of functional recovery of quantal release after more than one exposure to BoNT/A. We therefore investigated the recovery of quantal content in the ETA muscles after two and three injections, given at intervals of roughly 3–4 months (Fig. 12). In each case, the standard BoNT/A injection initially caused a rapid and profound block of quantal release.

Quantal release recovered significantly after both two and three injections, but more slowly than after a single injection. The slope of the regression line for recovery after a single injection was 0.89 quantal units day^{-1}. The slopes of the regression lines for recovery after two or three injections were not significantly different from each other. When these data were pooled, the slope of the regression for recovery after more than one injection was one-third of that for recovery after a single injection (0.30 quantal units day^{-1}). On the basis of these regression lines, the time for the quantal content to reach 50% of its normal value (57.9) was 43 days for one injection, 74 for two and 105 for three.

The statistical strength of these conclusions was tested using ANCOVA. The outcomes of this analysis are: (1) the regressions of the three groups (1, 2 and 3 injections) are not homogeneous ($P = 0.018$), (2) the regressions of the data for two and three injections are not significantly different, (3) the regression of the data for one injection is significantly different from that for either two ($P < 0.0001$) or three ($P << 0.0001$) injections, and (4) the regression of the data for one injection is significantly different from that for the pooled data for two and three injections ($P << 0.0001$). It is thus clear that in these experiments, recovery of evoked quantal release after an injection of BoNT/A was significantly slower in those mice that had received one or two previous injections.

Structural abnormalities persist after multiple BoNT/A injections. Although no systematic studies have been made, available evidence indicates that structural abnormalities of motor innervation persist in humans for years after the last of a series of BoNT/A injections (Alderson *et al.* 1991). We were therefore interested to see whether NMJs in the mouse ETA whose function had recovered after two or three BoNT/A injections showed similarly persistent structural abnormalities. In spite of the clear functional recovery, the abnormalities of the anatomical features of motor innervation were still present months after a second or, as illustrated in Fig. 13, a third injection.

At low magnifications, it was clear that the central band of innervation was much wider in injected muscles than in uninjected contralateral controls (Fig. 13*A* and *C*). In the examples illustrated (uninjected control and 124 days after BoNT/A) the innervation band is more than twice as wide as normal, and this was typical of the muscles we observed. We did not attempt to quantify this increase in detail, or to establish whether the width increased progressively with the number of injections.

At higher magnification, it was clear that the individual NMJs were also often very abnormal. Some examples from muscles at 124 days after a third injection of BoNT/A are shown in Fig. 13*D*–*G*. These show both persisting individual sprouts (Fig. 13*D*) and multiple lateral sprouts (Fig. 13*F* and *G*). At longer times after the final injection of BoNT/A (223 days), a number of very abnormal NMJs persisted (Fig. 13*H*–*K*). These were often associated with lateral branches of long myelinated axons coursing along the muscle fibres (Fig. 13*I*). Although NMJs from uninjected contralateral muscles were often rather complex (Fig. 13*B*), probably a result of the

21 days previously. Note great variation of both amplitude and time course, and much smaller amplitude than in control. *C* and *D*, changes in mean value of EPP_{in} rise time (*C*, 'RT') and decay time (*D*, 'DT') during recovery from BoNT/A. The total quantal content is shown in each graph for comparison. Note that the kinetic properties of the EPP_{in} return to normal values when the total quantal content has only reached approximately one-third of its normal value. *E*, variable time courses of EPP_{in}s recorded from the same muscle fibre, 15 days after exposure to BoNT/A. EPP_{in}s of two quite distinct time courses could be recorded from this fibre. Examples of these are shown in *F* (fast EPP_{in}s), *G* (mixed time-course EPP_{in}s) and *H* (slow EPP_{in}s). A single response showing both fast and slow components is highlighted in *G*.

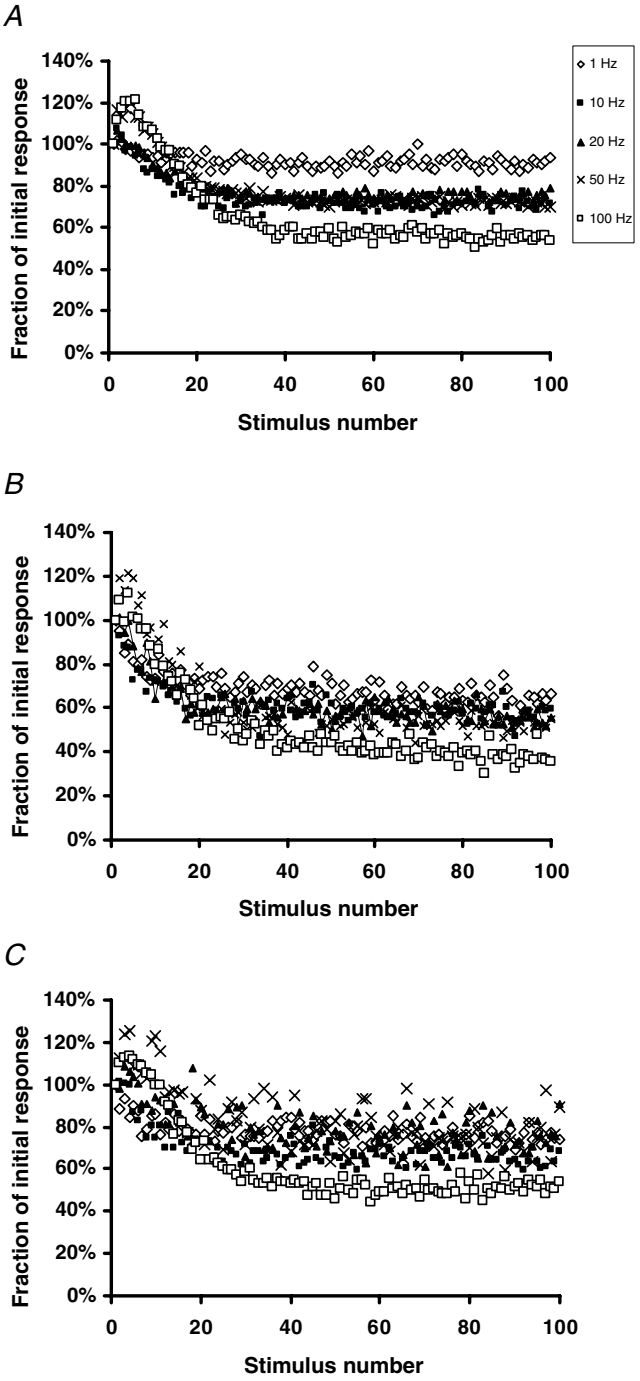

Figure 11. Response to repetitive stimulation of uninjected control NMJs and NMJs 4 months after recovery from BoNT/A
In each case trains of 100 stimuli were given at frequencies from 1 to 100 Hz and the peak amplitudes of the resulting EPP_{in}s are plotted. For both control (*A*) and recovered (*B* and *C*) NMJs, stimulation at 50 and 100 Hz caused initial facilitation followed by substantial depression. At 1–20 Hz, there was depression but no facilitation. The graphs show averaged pooled data from 75 NMJs from 5 uninjected control mice (*A*), from 45 NMJs from 3 mice 4 months after a single injection (*B*), and from 45 NMJs from 3 mice after a 2nd injection, given 4 months after the first (*C*).

advanced age (476 days) (Barker & Ip, 1966; Tuffery, 1971; Cardasis & LaFontaine, 1987), they only rarely had sprouts.

In summary, it is clear that although substantial recovery of quantal release occurs in ETA muscles after two or three injection of BoNT/A, striking structural abnormalities of the motor axons and NMJs may persist for many months.

Discussion

Summary of main results

An important finding of our study of the mouse ETA is that the region of the original NMJ plays a much greater role in the initial recovery from the blocking effects of BoNT/A than previously thought. In fact, our estimates of quantal release from new synaptic contacts suggest that they play a relatively minor role in functional recovery. A second important finding is that after several exposures to BoNT/A, while neuromuscular transmission can be restored to near normal levels, it does so more slowly than after a single exposure and is accompanied by profound abnormalities in the structure of the intramuscular nerve and the NMJs. These findings raise some concerns about the cumulative effects of repeated exposure to BoNT/A in a therapeutic or cosmetic context. At the same time, they attest to the remarkable adaptive plasticity of the mammalian NMJ.

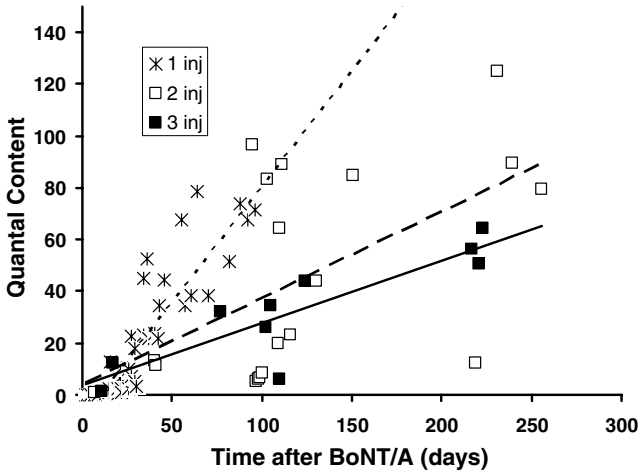

Figure 12. Recovery of quantal content at mouse ETA NMJs after one, two or three injections of BoNT/A
Injections were given at intervals of 3–4 months. Time is shown after the final injection. Note that recovery after 2 and 3 injections is slower than after a single injection. Each point indicates averaged values of pooled data from a number of fibres, typically 10, in one mouse. Regression lines have been drawn through the data for each number of injections: dotted, 1 injection; dashed, 2 injections; continuous, 3 injections. Statistical analysis is described in the text.

Initial recovery

Timing of recovery. The time course of recovery of quantal release after administration of BoNT/A is similar in the ETA to that described for sternomastoid (de Paiva *et al.* 1999) but is somewhat faster than that reported for other mouse muscles (soleus, EDL, LAL) where quantal content reached 50% of its normal value in 10–14 weeks

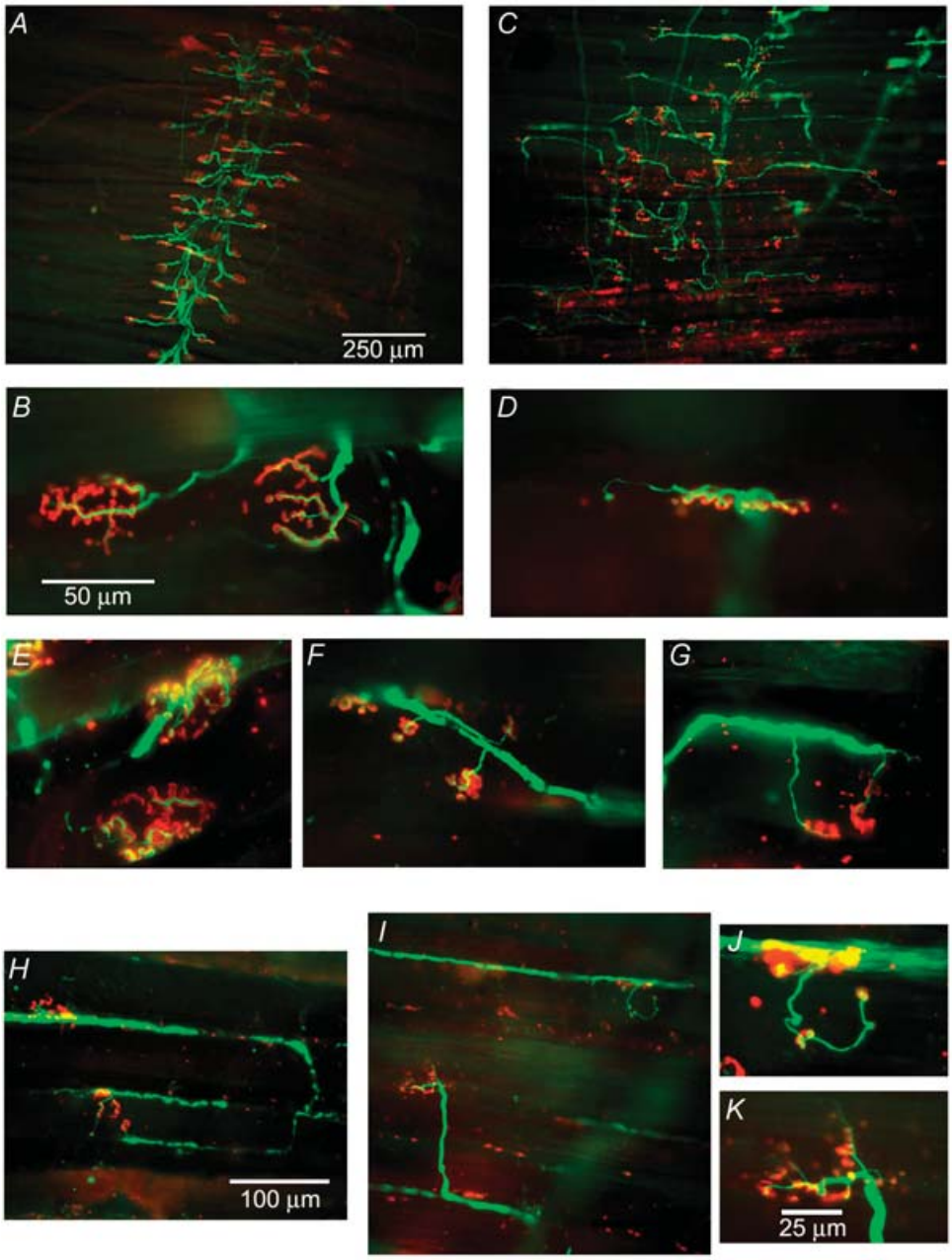

Figure 13. Abnormal structural aspects of motor innervation after three injections of BoNT/A
Nerves (green) immunolabelled with anti-NFP and anti-synaptophysin, AChR (red) labelled with R-BgTx). *A* and *C*, low magnification (scale bar in *A* also applies to *C*) views of normal (saline injected) ETA and an ETA from a mouse of approximately the same age (476 days) which had received 3 injections of BoNT/A at approximately 3-monthly intervals. The band containing NMJs is about twice as wide as normal indicating persisting abnormal distribution of NMJs. *B* and *D–G*, higher magnification views (scale bar in *B* applies to all 5 panels). *B* is from an uninjected muscle showing NMJ structure typical of mice of this age, consisting of a compact cluster of spot-like regions. *D–G* show a selection of NMJs from injected muscles, 124 days after the 3rd injection. While the NMJ in *E* has a structure within the normal range, the others show synaptic spots arising from ultraterminal sprouts (*D*) or short lateral axonal branches (*F* and *G*) that are very rarely seen in normal muscles. *H–K*, ETA muscle 223 days after 3rd injection of BoNT/A. The lower magnification views (*H* and *I*, same magnification) show axons coursing along the muscle fibres while the higher magnification views (*J* and *K*, same magnification) show abnormal distributions of AChR clusters.

(Tonge, 1974; Santafe *et al.* 2000). In making these comparisons, it is important to bear in mind that different preparations of BoNT/A were used, and possibly different effective doses, and that different methods were used to estimate quantal content. In spite of these differences, the time required for all these mouse muscles to recover after BoNT/A is roughly similar to the duration of effectiveness of a single injection in man. It should be noted, however, that because of the high safety factor for neuromuscular transmission (Wood & Slater, 2001), patients may sense significant functional recovery when transmission is still substantially depressed. What of course differs between mice and men is the fraction of the lifespan required for recovery.

Several studies have noticed the 'weaker' sprouting response evoked by BoNT/A in functionally fast muscles (Duchen, 1970; Brown *et al.* 1980; Caroni *et al.* 1997; Frey *et al.* 2000). It is reasonable to suppose that that the pattern of short, high frequency bursts characteristic of fast motor units (Hennig & Lomo, 1985), which is known to be particularly effective in suppressing many effects of muscle inactivity (Windisch *et al.* 1998), might also suppress axonal sprouting and thus hinder recovery from BoNT/A (Brown *et al.* 1980). However, it is clear from both our observations of the ETA and previous studies of the LAL (Juzans *et al.* 1996*a*) that rapid and extensive sprouting can occur in an almost exclusively fast muscle, and that functional recovery can also be relatively fast. As discussed below, one possible explanation for this may be that fast muscles tend to make new sprouts within the area of the original NMJ.

Contribution of new synaptic contacts to recovery. Our conclusions concerning the role of new synaptic contacts to functional recovery from BoNT/A differ substantially from those of the only previous study to investigate this point (de Paiva *et al.* 1999; Meunier *et al.* 2003). Because the conclusions of that study have been cited in a number of subsequent articles (Meunier *et al.* 2002; Foran *et al.* 2003; Dolly & Aoki, 2006; Osborne *et al.* 2007), it is important to consider the possible origins of these differences.

de Paiva *et al.* (1999) used FM1-43 uptake to assess nerve terminal function. In many situations, a good correspondence between the intensity of FM1-43 labelling and quantal release has been demonstrated (Cochilla *et al.* 1999). However, in the present situation, this method has certain limitations. One is its inherent sensitivity. During the early stages of recovery after BoNT/A, the intensity of quantal release we observed at the sites of the original NMJs is only a few per cent of normal. While electrophysiological recording is capable of detecting the effects of individual quanta, the fluorescence signals associated with such low levels of release would be difficult to detect. Further, it is important to note that the lowest levels of FM1-43 labelling of the original terminals documented by de Paiva *et al.* remained at 10–25% of the normal value (see their Fig. 1*h*; de Paiva *et al.* 1999). However in studies, including the present one, where quantal release has been measured directly, it has initially fallen to less than 1% of normal. This suggests that the intensity of FM1-43 fluorescence may not accurately reflect the low levels of quantal release that follow BoNT/A intoxication.

An important further assumption made by de Paiva *et al.* 1999 is that the FM1-43 signal from the entire length of the sprouts reflects physiologically significant transmitter release. Only transmitter quanta released within a few micrometres of AChR clusters can have any impact on membrane excitation. However, it is clear from de Paiva *et al.* and from this study that AChR clusters occupy only a small fraction of the total length of the sprouts (cf. Figs 3 and 13). Thus, while membrane cycling may occur all along the sprouts as they grow and extend lateral branches, much of this may not be relevant for quantal release of ACh. Our electrophysiological approach, while not measuring ACh release directly, does indicate 'effective' release, i.e. that which leads to membrane depolarization.

The influence of terminal sprouting on quantal release from the mammalian NMJs has been investigated in another context, that of recovery after chronic block of nerve impulses. Using a cuff containing tetrodotoxin to block the rat sciatic nerve, Tsujimoto *et al.* (1990) observed an increase in quantal content before any sprouting was detectable. At later times, the quantal content was no greater at those NMJs where sprouting had occurred than where it had not. They concluded that sprouting and increased quantal content are not causally related in the conditions of their experiments. By implication, a mechanism must exist by which quantal content can be raised within the confines of the original NMJ. A similar conclusion was reached in studies of increased quantal release in the absence of any enlargement of the NMJ in myasthenia gravis and an animal model of it (Plomp *et al.* 1992, 1995). The mechanism of the up-regulation of quantal release in these situations is unknown. It is therefore impossible to know whether a similar mechanism might be responsible for the recovery of the original NMJs after exposure to BoNT/A. However, it should be noted that in these other examples there is no indication of structural alterations to the proteins involved in exocytosis, or to the resulting need to replace them, that characterize the response to BoNT/A.

Changes in synaptic events during recovery. Previous studies of NMJs blocked by BoNT/A have reported an increase in the number of spontaneous mEPPs with abnormally large amplitudes and long time courses (Thesleff & Molgo, 1983; Kim *et al.* 1984), sometimes referred to as 'giant' or 'slow' mEPPs. Much less has been reported about the properties of evoked EPPs and EPCs. While it has been stated that the rise time of individual

evoked EPPs remained normal during the recovery period (Kim *et al.* 1984), evidence has also been presented of a slowing of the decay phase of EPCs 1 week after exposure to BoNT/A (Sellin & Thesleff, 1981). In the present study we observed a striking slowing of the time course of the evoked responses recorded during recovery. This slowing resulted from increases in the latency, synaptic delay and the rise and decay times of the EPPs. These changes reached a peak just as transmission began to be effective and were largely reversed when the quantal content was still only 20–30% of normal. It may be that these changes were missed in earlier studies which concentrated more on changes in the first week after exposure to BoNT/A.

The nature of these changes in EPP time course is likely to be multifactorial. Both the prolonged synaptic delay and the slower rise time of the EPP suggest alterations of the release process. These may well be related to recovery from the effects of the cleavage of SNAP-25 (Sakaba *et al.* 2005). In addition, there is evidence that during recovery from BoNT/A, L- and N-type voltage-gated calcium channels are present in the nerve terminal along with the P/Q-type channels normally present (Day *et al.* 1997; Santafe *et al.* 2000; Pagani *et al.* 2004). It is possible that the L- and N-type channels are not as closely associated with the active zone (Urbano *et al.* 2003) as the P/Q-channels and this may lead to an increase in latency and/or rise time of the EPP. Little is known about the sequence of events in this process of nerve terminal maturation or how it is regulated.

On the postsynaptic side, the period of inactivity imposed by the action of BoNT/A almost certainly results in reduction of AChE activity (Hall, 1973) at the original synaptic sites and increase in the expression of γ-AChR subunits and hence slow, 'fetal' AChRs (Klarsfeld & Changeux, 1985; Goldman *et al.* 1988; Witzemann *et al.* 1991; Koltgen *et al.* 1994; Missias *et al.* 1996). Both of these postsynaptic changes would be likely to lead to the prolongation of the falling phase of the EPP. However, they would not be expected to have a major impact on the rising phase. AChE appears at new synaptic sites soon after the sprouts grow out (Duchen, 1970) and would be expected to hasten the falling phase of synaptic currents and potentials at the new sites. How, if at all, the slow EPPs we observed correspond to the slow mEPPs reported previously is unclear. Although we found a correlation between the time courses of EPPs and mEPPs from the same fibres, the numbers of mEPPs was too small to be confident of this relationship.

It was particular striking that more than one population of EPPs could be recorded from some single muscle fibres (Fig. 10). The very slow rise time of the 'slow' components strongly suggests local variations in the properties of the nerve terminals. It may be that the various synaptic spots, potentially both new and old, on a given muscle fibre acquire 'mature' properties at different times. The increase in quantal content associated with recovery of the ETA lasts at least 8–10 weeks. Previous studies have shown that axonal sprouts may continue to grow for a similar length of time (Juzans *et al.* 1996*a*; Santafe *et al.* 2000). It is therefore likely that new contacts continue to be made throughout this period, though possibly at a progressively slower rate as muscle activity returns to normal. This suggests that synaptic contacts established both early and late in the recovery process might coexist on the same muscle fibre, and might have relatively fast and slow EPPs associated with them.

By the end of the main recovery process, 3–4 months after exposure to BoNT/A, the functional properties of mouse ETA NMJs that we examined had essentially returned to normal. The observation that the response to repetitive stimulation is qualitatively similar to that in untreated mice, showing both rapid transient potentiation at high frequency followed by depression, suggests that both calcium dynamics and synaptic vesicle pools in the motor nerve terminals recover their normal properties after treatment with BoNT/A. Not enough experiments of this kind were performed to know whether the differences between the curves in Fig. 11 represent statistically significant differences.

Recovery from multiple exposures to BoNT/A

Ours is the only study we are aware of that has examined systematically the state of neuromuscular transmission after multiple exposures to BoNT/A. Although the extended duration of these experiments means that the samples were not large, it is nonetheless clear that very substantial recovery is possible even after three exposures. This is consistent with the clinical observations that underlie the need for multiple injections to maintain effective weakening of dystonic muscles (Jankovic & Hallett, 1994). However, there is a clear indication from our data that recovery after two and three exposures is slower, and more variable, than after an initial exposure.

In contrast to the eventual success of functional recovery, striking structural abnormalities persisted long after multiple exposures to BoNT/A. This indicates that, at least in the mouse ETA, an appreciable number of the new contacts made during initial recovery survive the withdrawal process that has been noted by previous authors (Duchen, 1970; de Paiva *et al.* 1999). Whether the plasticity of these 'extended' nerve branches when confronted with further exposures to BoNT/A is as great as when BoNT/A is first given is unclear. It is also important to note that the animals receiving multiple injections were generally older when the muscles were examined than those receiving only one. How, if at all, the ageing process influences NMJ plasticity remains an important question for the future.

Biological and clinical implications

Our results indicate that recovery of evoked quantal release can occur in the region of the original NMJ at an early stage of the response to BoNT/A. In addition, they show that there are similarities in the sequence of events in the maturation of the release process at the original NMJ and at more remote 'new' contacts. The structural basis of the early release we observed from the region of the original NMJ is not clear. One possibility is that the original contacts recover more rapidly than previously thought. Alternatively, or in addition, it may be that new sprouts and functional contacts are made within the original synaptic region as well as more remotely. Local remodelling of the NMJ is well-documented in a number of situations. It occurs during normal ageing (Barker & Ip, 1966; Arizono *et al.* 1984) and is very marked at NMJs on muscle fibres that regenerate after damage (Duchen *et al.* 1974; Lyons & Slater, 1991). Although the molecular basis of this local plasticity is not understood in detail, up-regulation of surface adhesion molecules is likely to play a part. In support of this is the observation that overexpression of NCAM in mouse muscle leads to sprouting both within and away from the NMJs (Walsh *et al.* 2000). Since muscle inactivity leads to up-regulation of NCAM (Cashman *et al.* 1987), it is likely to occur after exposure to BoNT/A and may therefore play an important part in stimulating both local and remote sprouting. If, as seems likely from available evidence (Duchen, 1970; Brown *et al.* 1980; Frey *et al.* 2000), the detailed pattern of recovery differs between species and muscles, it will be of interest to learn which factors determine the balance between reinnervation of the original NMJ and the formation of new, often quite remote, synaptic contacts in different muscles.

A striking feature of NMJ remodelling is that it often results in NMJs with abnormal structure but substantially normal function. This is known to be true in two of the examples cited above (*mdx* mice, NCAM up-regulation). The ability of the NMJ to maintain an adequately functional state in the face of structural disruption is further supported by observations of NMJs after multiple exposures to BoNT/A both in animals, as presented here, and in humans (Holds *et al.* 1990) (Pang *et al.* in preparation). Together with other evidence of the ability of the mammalian NMJ to regulate quantal output to match need (e.g. Plomp *et al.* 1994, 1995), these findings attest to the remarkable adaptive plasticity of the NMJ. In spite of its biological importance, almost nothing is known about the nature of this form of plasticity.

Although we found that NMJs in the mouse ETA could recover function after multiple exposures to BoNT/A, there was clear indication that the process eventually became less effective. Thus, there was an accumulation of structurally abnormal NMJs and functional recovery was slower after an initial exposure. These observations suggest that the NMJ does not return to a fully normal state after repeated exposure to BoNT/A. This should sound a note of caution for those using BoNT/A as the basis for clinical and cosmetic treatments.

References

Alderson K, Holds JB & Anderson RL (1991). Botulinum-induced alteration of nerve–muscle interactions in the human orbicularis oculi following treatment for blepharospasm. *Neurology* **41**, 1800–1805.

Angaut-Petit D, Molgo J, Comella JX, Faille L & Tabti N (1990). Terminal sprouting in mouse neuromuscular junctions poisoned with botulinum type A toxin: morphological and electrophysiological features. *Neuroscience* **37**, 799–808.

Arizono N, Koreto O, Iwai Y, Hidaka T & Takeoka O (1984). Morphometric analysis of human neuromuscular junction in different ages. *Acta Pathol Japon* **34**, 1243–1249.

Barker D & Ip MC (1966). Sprouting and degeneration of mammalian motor axons in normal and de-afferentated skeletal muscle. *Proc Roy Soc Lond B Biol Sci* **163**, 538–554.

Bradley SA, Lyons PR & Slater CR (1989). The epitrochleoanconeus muscles (ETA) of the mouse: a useful muscle for the study of motor innervation. *J Physiol* **415**, 3*P*.

Brigant JL & Mallart A (1982). Presynaptic currents in mouse motor endings. *J Physiol* **333**, 619–636.

Brown MC, Holland RL & Ironton R (1980). Nodal and terminal sprouting from motor nerves in fast and slow muscles of the mouse. *J Physiol* **306**, 493–510.

Cardasis CA & LaFontaine DM (1987). Aging rat neuromuscular junctions: a morphometric study of cholinesterase-stained whole mounts and ultrastructure. *Muscle Nerve* **10**, 200–213.

Caroni P, Aigner L & Schneider C (1997). Intrinsic neuronal determinants locally regulate extrasynaptic and synaptic growth at the adult neuromuscular junction. *J Cell Biol* **136**, 679–692.

Cashman NR, Covault J, Wollman RL & Sanes JR (1987). Neural cell adhesion molecule in normal, denervated, and myopathic human muscle. *Ann Neurol* **21**, 481–489.

Cochilla AJ, Angleson JK & Betz WJ (1999). Monitoring secretory membrane with FM1-43 fluorescence. *Annu Rev Neurosci* **22**, 1–10.

Day NC, Wood SJ, Ince PG, Volsen SG, Smith W, Slater CR & Shaw PJ (1997). Differential localization of voltage-dependent calcium channel alpha1 subunits at the human and rat neuromuscular junction. *J Neurosci* **17**, 6226–6235.

del Castillo J & Katz B (1954). Quantal components of the end-plate potential. *J Physiol* **124**, 560–573.

del Castillo J & Katz B (1956). Localization of active spots within the neuromuscular junction of the frog. *J Physiol* **132**, 630–649.

de Paiva A, Meunier FA, Molgo J, Aoki KR & Dolly JO (1999). Functional repair of motor endplates after botulinum neurotoxin type A poisoning: biphasic switch of synaptic activity between nerve sprouts and their parent terminals. *Proc Natl Acad Sci U S A* **96**, 3200–3205.

Dolly JO & Aoki KR (2006). The structure and mode of action of different botulinum toxins. *Eur J Neurol* **13** (Suppl. 4), 1–9.

Dong M, Yeh F, Tepp WH, Dean C, Johnson E, Janz R & Chapman ER (2006). SV2 is the protein receptor for botulinum neurotoxin A. *Science* **312**, 592–596.

Duchen LW (1970). Changes in motor innervation and cholinesterase localization induced by botulinum toxin in skeletal muscle of the mouse: differences between fast and slow muscles. *J Neurol Neurosurg Psychiatry* **33**, 40–54.

Duchen LW, Excell BJ, Patel R & Smith B (1974). Changes in motor end-plates resulting from muscle fibre necrosis and regeneration. A light and electron microscopic study of the effects of the depolarizing fraction (cardiotoxin) of *Dendroaspis jamesoni* venom. *J Neurol Sci* **21**, 391–417.

Foran PG, Davletov B & Meunier FA (2003). Getting muscles moving again after botulinum toxin: novel therapeutic challenges. *Trends Mol Med* **9**, 291–299.

Frey D, Schneider C, Xu L, Borg J, Spooren W & Caroni P (2000). Early and selective loss of neuromuscular synapse subtypes with low sprouting competence in motoneuron diseases. *J Neurosci* **20**, 2534–2542.

Goldman D, Brenner HR & Heinemann S (1988). Acetylcholine receptor α-, β-, γ-, and d-subunit mRNA levels are regulated by muscle activity. *Neuron* **1**, 329–333.

Hall ZW (1973). Multiple forms of acetylcholinesterase and their distribution in endplate and non-endplate regions of rat diaphragm muscle. *J Neurobiol* **4**, 343–361.

Hennig R & Lomo T (1985). Firing patterns of motor units in normal rats. *Nature* **314**, 164–166.

Holds JB, Alderson K, Fogg SG & Anderson RL (1990). Motor nerve sprouting in human orbicularis muscle after botulinum A injection. *Invest Ophthalmol Vis Sci* **31**, 964–967.

Jankovic J & Hallett M (1994). *Therapy with Botulinum Toxin*. Marcel Dekker, Inc., New York.

Juzans P, Comella JX, Molgo J, Faille L & Angaut-Petit D (1996*a*). Nerve terminal sprouting in botulinum type-A treated mouse levator auris longus muscle. *Neuromuscul Disord* **6**, 177–185.

Juzans P, Molgo J, Faille L & Angaut-Petit D (1996*b*). Synaptotagmin II immunoreactivity in normal and botulinum type-A treated mouse motor nerve terminals. *Pflugers Arch* **431**, R283–R284.

Katz B (1969). *The Release of Neural Transmitter Substances*. Liverpool University Press, Liverpool.

Katz B & Miledi R (1965). Propagation of electric activity in motor nerve terminals. *Proc R Soc Lond B Biol Sci* **161**, 453–482.

Kim YI, Lomo T, Lupa MT & Thesleff S (1984). Miniature end-plate potentials in rat skeletal muscle poisoned with botulinum toxin. *J Physiol* **356**, 587–599.

Klarsfeld A & Changeux JP (1985). Activity regulates the levels of acetylcholine receptor α-subunit mRNA in cultured chicken myotubes. *Proc Natl Acad Sci U S A* **82**, 4558–4562.

Koltgen D, Ceballos-Baumann AO & Franke C (1994). Botulinum toxin converts muscle acetylcholine receptors from adult to embryonic type. *Muscle Nerve* **17**, 779–784.

Liley AW (1956). An investigation of spontaneous activity at the neuromuscular junction of the rat. *J Physiol* **132**, 650–666.

Lyons PR & Slater CR (1991). Structure and function of the neuromuscular junction in young adult mdx mice. *J Neurocytol* **20**, 969–981.

Magrassi L, Purves D & Lichtman JW (1987). Fluorescent probes that stain living nerve terminals. *J Neurosci* **7**, 1207–1214.

Mallart A & Brigant JL (1982). Electrical activity at motor nerve terminals of the mouse. *J Physiol (Paris)* **78**, 407–411.

Martin AR (1955). A further study of the statistical composition of the end-plate potential. *J Physiol* **130**, 114–122.

McLachlan EM & Martin AR (1981). Non-linear summation of end-plate potentials in the frog and mouse. *J Physiol* **311**, 307–324.

Meunier FA, Lisk G, Sesardic D & Dolly JO (2003). Dynamics of motor nerve terminal remodeling unveiled using SNARE-cleaving botulinum toxins: the extent and duration are dictated by the sites of SNAP-25 truncation. *Mol Cell Neurosci* **22**, 454–466.

Meunier FA, Schiavo G & Molgo J (2002). Botulinum neurotoxins: from paralysis to recovery of functional neuromuscular transmission. *J Physiol (Paris)* **96**, 105–113.

Missias AC, Chu GC, Klocke BJ, Sanes JR & Merlie JP (1996). Maturation of the acetylcholine receptor in skeletal muscle: regulation of the AChR gamma-to-epsilon switch. *Dev Biol* **179**, 223–238.

Molgo J, Comella JX, Angaut-Petit D, Pecot-Dechavassine M, Tabti N, Faille L, Mallart A & Thesleff S (1990). Presynaptic actions of botulinal neurotoxins at vertebrate neuromuscular junctions. *J Physiol (Paris)* **84**, 152–166.

Osborne SL, Latham CF, Wen PJ, Cavaignac S & Fanning Je (2007). The janus faces of botulinum neurotoxin: Sensational medicine and deadly biological weapon. *J Neurosci Res* **85**, 1149–1158.

Pagani R, Song M, McEnery M, Qin N, Tsien R & We (2004). Differential expression of α1 and β subunits of voltage dependent Ca^{2+} channel at the neuromuscular junction of normal and P/Q Ca^{2+} channel knockout mouse. *Neuroscience* **123**, 75–85.

Pang K, Quinby J, Eyre J & Slater C (2002). The neuromuscular junction in cerebral palsy and its response to botulinum toxin-A. *Dev Med Child Neurol* **43** (Suppl. 90), 13.

Plomp JJ, van Kempen GT, De Baets MB, Graus YM, Kuks J & Be (1995). Acetylcholine release in myasthenia gravis: regulation at single end-plate level. *Ann Neurol* **37**, 627–636.

Plomp JJ, van Kempen GT & Molenaar PC (1992). Adaptation of quantal content to decreased postsynaptic sensitivity at single endplates in α-bungarotoxin-treated rats. *J Physiol* **458**, 487–499.

Plomp JJ, van Kempen GT & Molenaar PC (1994). The upregulation of acetylcholine release at endplates of α-bungarotoxin-treated rats: its dependency on calcium. *J Physiol* **478**, 125–136.

Sakaba T, Stein A, Jahn R & Neher E (2005). Distinct kinetic changes in neurotransmitter release after SNARE protein cleavage. *Science* **309**, 491–494.

Santafe MM, Urbano FJ, Lanuza MA & Uchitel OD (2000). Multiple types of calcium channels mediate transmitter release during functional recovery of botulinum toxin type A-poisoned mouse motor nerve terminals. *Neuroscience* **95**, 227–234.

Schiavo G, Matteoli M & Montecucco C (2000). Neurotoxins affecting neuroexocytosis. *Physiol Rev* **80**, 717–766.

Sellin LC & Thesleff S (1981). Pre- and post-synaptic actions of botulinum toxin at the rat neuromuscular junction. *J Physiol* **317**, 487–495.

Slater CR, Lyons PR, Walls TJ, Fawcett PR & Young C (1992). Structure and function of neuromuscular junctions in the vastus lateralis of man. A motor point biopsy study of two groups of patients. *Brain* **115**, 451–478.

Slater CR & Rogozhin AA (2006). Do newly formed synaptic contacts account for functional recovery from botulinum toxin type A? *Neurotoxicity Res* **9**, 221.

Thesleff S & Molgo J (1983). A new type of transmitter release at the neuromuscular junction. *Neuroscience* **9**, 1–8.

Thesleff S, Molgo J & Lundh H (1983). Botulinum toxin and 4-aminoquinoline induce a similar abnormal type of spontaneous quantal transmitter release at the rat neuromuscular junction. *Brain Res* **264**, 89–97.

Tonge DA (1974). Chronic effects of botulinum toxin on neuromuscular transmission and sensitivity to acetylcholine in slow and fast skeletal muscle of the mouse. *J Physiol* **241**, 127–139.

Tsujimoto T, Umemiya M & Kuno M (1990). Terminal sprouting is not responsible for enhanced transmitter release at disused neuromuscular junctions of the rat. *J Neurosci* **10**, 2059–2065.

Tuffery AR (1971). Growth and degeneration of motor end-plates in normal cat hind limb muscles. *J Anat* **110**, 221–247.

Urbano FJ, Piedras-Renteria ES, Jun K, Shin HS & De Uchitel O, (2003). Altered properties of quantal neurotransmitter release at endplates of mice lacking P/Q-type Ca^{2+} channels. *Proc Natl Acad Sci U S A* **100**, 3491–3496.

Walsh FS, Hobbs C, Wells DJ, Slater CR & Fazeli S (2000). Ectopic expression of NCAM in skeletal muscle of transgenic mice results in terminal sprouting at the neuromuscular junction and altered structure but not function. *Mol Cell Neurosci* **15**, 244–261.

Windisch A, Gundersen K, Szabolcs MJ, Gruber H & Lomo T (1998). Fast to slow transformation of denervated and electrically stimulated rat muscle. *J Physiol* **510**, 623–632.

Witzemann V, Brenner HR & Sakmann B (1991). Neural factors regulate AChR subunit mRNAs at rat neuromuscular synapses. *J Cell Biol* **114**, 125–141.

Wood SJ & Slater CR (1997). The contribution of postsynaptic folds to the safety factor for neuromuscular transmission in rat fast- and slow-twitch muscles. *J Physiol* **500**, 165–176.

Wood SJ & Slater CR (2001). Safety factor at the neuromuscular junction. *Prog Neurobiol* **64**, 393–429.

Yee WC & Pestronk A (1987). Mechanisms of postsynaptic plasticity: remodeling of the junctional acetylcholine receptor cluster induced by motor nerve terminal outgrowth. *J Neurosci* **7**, 2019–2024.

Acknowledgements

We thank Leo Gurney, Helen Fairley and Julie Coaker for participating in some of the early experiments and data analysis. We thank The Wellcome Trust for the principal financial support of this project, and grant 4177.2008.4 from The President of the Russian Federation for Leading Scientific Schools for further support. We thank Allergan, Ltd for providing gratis the BOTOX® used in this project.